Radiochim. Acta **100**, 329–338 (2012) / **DOI** 10.1524/ract.2012.1918

Impact of water environmental change and migration of radionuclides on Hokutolite conservation in Peito (Taiwan)

By C.-C. Lin[1,*], T.-L. Tsai[2] and C.-C. Lung[3]

[1] Department of Natural Biotechnology/Institute of Natural Healing Sciences/General Education Center, Nanhua University, No. 55, Nanhua Rd., Dalin, Chia-Yi 62248, Taiwan
[2] Chemical Analysis Division, Institute of Nuclear Energy Research, Longtan 32546, Taiwan
[3] Department of Public Health, Chung-Shan Medical University, Taichung, 402 Taiwan

(Received April 20, 2011; accepted in revised form September 19, 2011)
(Published online March 12, 2012)

Water environment / Hokutolite / Hot spring / Migration / Peito / Disequilibrium

Summary. Chemical factors (including pH, redox potential, content of total organic compound (TOC) and major ions) and U/Th-series radionuclides in the hot-spring water environment of Peito were determined to investigate the impact of environmental change and migration of radionuclides in water on conserving the precious mineral, hokutolite, in Peito (Taiwan). The activity concentrations of U/Th increased with E_h and those of Cl^- and SO_4^{2-}. $^{234}U/^{238}U$ ratios were nearly > 1 ascribed to Szilárd–Chalmers effect and α-recoil. $^{230}Th/^{234}U$ ratios were < 1 resulting from complexation with chloride and sulfate ions. ^{228}Ra and ^{226}Ra activities were governed by pH, E_h and SO_4^{2-} concentration. Disequilibria of $^{228}Th/^{228}Ra$ and $^{228}Ra/^{232}Th$ were evident attributed to complexation of Th with major anions and co-precipitation of radium with $(Ba,Pb)SO_4$. Alpha-recoil caused the enrichment of ^{228}Ra and apparent disequilibrium of $^{232}Th/^{228}Th$. A mechanism illustrating the radiochemistry involving the formation of hokutolite in Peito was derived accordingly. The water environment of the studied area was found apparently changed in light of the variation of temperature, TOC and concentration ratio of Ba/Pb, which resulted from the channeling of hot spring water and the release of household waste water. The water environmental change can thus hinder the migration of radionuclides as well as the formation of hokutolite so that the performance of hokutolite conservation can be decreased. Immediate enactment of regulations for conserving hokutolite in Peito was therefore suggested in this research.

1. Introduction

The Peito Hot Spring Area is located in Peito of Taipei city in Taiwan (Fig. 1), of which the stratum (Wuzhi Mountain layer) developed after Miocene composes principally andesite and basalt [1]. Since the discovery of hokutolite (which is also named as Peito stone) in Peito Creek by Yohachiro Okamoto in 1905, the Peito (or Beitou) Hot Spring has become an illustrious scenic area [1, 2]. The Peito stone was named as anglesobarite by Hayakawa and Nakano in 1912 [3] and was renamed later as hokutolite by Jimbo [4] in 1913. Hokutolite has been regarded even more precious than gold, which is mainly composed of plumbian barite [$(Ba, Pb)SO_4$] in chemistry [5]. Hokutolite is celebrated for its radioactivity originating from radium and thorium precipitating from geothermal waters [6]. The spring water of the studied area is hot and achromatous with a strongly acidic odor, which cools as it flows into the creek. Hokutolite crystallized on the gravel bed of the Peito Creek at about 90–300 m downstream from the Geothermal Valley [1, 7]. Gravels in the Peito Creek near Peito Hot Spring Area were mostly of andesite deposited with rhombic tabular crystals in outer part and covered with a thin fibrous crust of hokutolite [8]. These glassy crystals were normally less than 10 mm in thickness with yellowish gray or brown color and a resinous luster.

Unfortunately, hokutolite was gathered illegally before 1997 due to powerless management. On the other hand, several SPA hotels were erected successively along the Peito Creek (Fig. 1) to provide hot spring bath and accommodations since 1960s. The geothermal water was channeled from underground reservoirs through drilling wells and pipelines to the SPA hotels and local residences. Tapwater was mixed the geothermal water for hot spring bath and then the waste water was discharged into the creek. Environment and ecology of the Peito Creek was seriously spoiled by human activities simultaneously on developing tourism of this area. Reconstruction of this area commenced in 1997 to recover hokutolite according to some appeals from local environmental organizations to the government. The conserved hokutolites were exhibited in Peito Hot Spring Museum opened on 11 October 1998. However, the channeling of spring water and discharge of waste water are still proceeding and thus affecting the water chemistry of the studied area. This may influence the recovery of hokutolite. In order to effectively recover the hokutolite in Peito, it is imperative to realize the mechanism for the formation of this precious mineral.

Radioactive disequilibria within U/Th-series radionuclides arisen from surface and near-surface processes have been a useful tool in dealing with diverse problems in environmental, geochemical and archaeological fields [9–19].

*Author for correspondence (E-mail: cclin@mail.nhu.edu.tw).

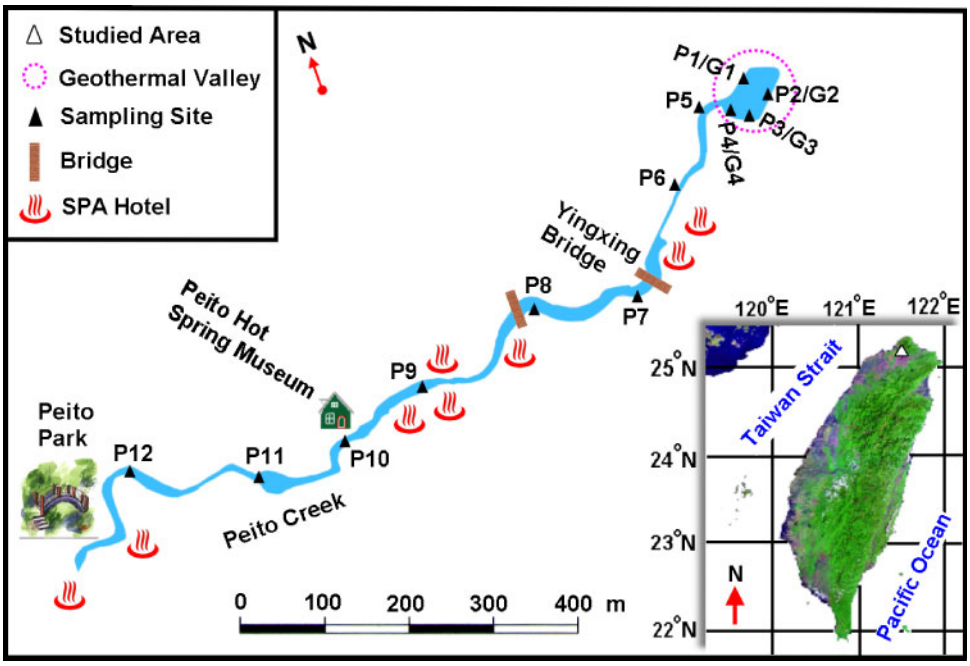

Fig. 1. Sampling sites located at the studied area of Northern Taiwan.

Prior studies about hokutolite and radioactive disequilibria in Peito were almost aiming at the Geothermal Valley where the springhead is located [2, 20–22]. Nevertheless, very few researches investigated the Peito Creek where hokutolite was produced. Literatures concerning the relationship between chemistry in water environmental and radioactive disequilibria of the Peito Hot Spring Area or hokutolite formation are also very limited. Additionally, the disequilibria were usually demonstrated physically with recoil, weathering and erosion perturbing the radioactive disequilibria in the environment [21]. However, the disequilibria between radionuclides with different chemical speciation (*e.g.*, U and Th isotopes) may involve chemical reactions and radionuclide migrations. Accordingly, related characteristics of the aqueous environment in the Peito Hot Spring Area were examined in this research to investigate their effects on migrations and radiochemical behaviors of radionuclides and further to interpret disequilibria of long-life U/Th-series radionuclides and the formation of hokutolite in Peito.

2. Experimental

2.1 Sample description

All samples were collected in the Peito Hot Spring Area where includes the Peito Creek and the Geothermal Valley (Fig. 1). Geothermal water was sampled in 20-L polyethylene containers from 12 different sites, including 4 spots in the Geothermal Valley and others along the Peito Creek. Sample P1/G1–P4/G4 specify water/sediment samples obtained from Geothermal Valley, where water channeling and waste water discharge are forbidden. Other sample codes, P5–P12, signify water samples collected from upstream toward downstream Peito Creek and were close to main discharge points. According to the literature [1], the distribution of hokutolite ranged principally from P6 to P10. The sediment was distributed mainly in Geothermal Valley, which was collected from G1–G4 at 10 cm deep.

2.2 Materials and methods

Digestion reagents including 65% HNO_3, 37% HCl and 48% HF (Merck Co., Germany) were of Suprapur® grade, which were also utilized for column conditioning and cation exchange in this work. A microwave device (Model MARS-5, CEM, Matthews, North Carolina, USA) was utilized in sample digestion with operation condition of 180 psi and 210 °C. A semiconducting surface barrier detector (Canberra model 7200-06) with a detection efficiency ranging from 20 to 25% and a resolution of less than 20 keV for 5.486 MeV of alpha particles from ^{241}Am was used for determining U and Th isotopes. Cations in water were determined with an inductively coupled plasma-atomic emission spectrometer (ICP-AES; Ultima Horiba Jobin Yvon). An ion chromatographer (Dionex AS12) was employed to determine the concentration of anions. Ultra-pure water obtained from a Milli-Q Gradient water purifier (Millipore, Billerica, MA, USA) was used for dilution throughout this work.

The temperature, acidity, and oxidation-reduction potential (E_h) were measured in situ with a portable meter (HI-8424, Hanna Instrument Co., USA) accessorized with a temperature probe (HI-7669 AW) and an electrode (HI-1230B) for pH and redox potential measurements. A multi-range conductivity meter (HI-8633N, Hanna Instrument Co., USA) was utilized to obtain the conductivity. An aliquot of water sample was carried with synthetic air (at a flow rate of 200 mL min^{-1} and a pressure of 1.0–1.2 bar) into a liqui-TOC II analyzer (Elementar Analysensysteme Hanau, Germany) for TOC (Total Organic Compounds) determination.

The radium and a ^{133}Ba purchased from NIST tracer were concentrated using AG 50W-X12 resin [23]. The eluate was evaporated to dryness, and the residue was dissolved in 0.1 M HCl. After scintillation cocktail containing 10 mL of the insoluble high efficiency mineral oil (Packard Instrument Co.) was added, the solution was sealed for 30 d to establish radioactive equilibrium between ^{226}Ra and ^{222}Rn. The ^{226}Ra radioactivity was determined by measuring ^{222}Rn in a low

activity liquid scintillation counter (Tri-Carb 2550 TR/AB, Packard Instrument Co., USA) equipped with a pulse-shape analyzer (PSA) which separated pulses caused by alpha or beta decays into different spectra.

After dried 24 h at 105 °C, the sediment was powdered and then sifted with a sieve of 60-mesh. To determine the activity concentration (nCi/kg) of ^{228}Ra by gamma spectrometry, the sediment was weighed and hermetically sealed in an plastic jar of 125 mL while the water was kept airtight in Marinelli beakers for 1 month to establish radioactive equilibrium between ^{228}Ra and ^{228}Ac [24].

Uranium and thorium isotopes (including ^{238}U, ^{234}U, ^{232}Th, ^{230}Th and ^{228}Th) in water or sediment were separated respectively using U/TEVA and TEVA resins, which were further determined by α spectrometry with a semiconducting surface barrier detector as developed in our previous study [25].

3. Results and discussion

3.1 Environmental characteristics of the sampling sites

Chemical parameters including pH, E_h, conductivity, temperature and concentrations of major anions (Cl^- and SO_4^{2-}) the geothermal water in the studied area are shown in Table 1. Acidity of the water decreased from the Geothermal Valley (P1/G1-P4/G4) toward downstream Peito Creek. Temperature, conductivity and redox potential varied similarly against sampling sites, which exhibited higher values in the Geothermal Valley (P1/G1-P4/G4) than those in the Peito Creek (P6–P12).

The pH values indicated that the geothermal water in this area was quite acidic, which favors acid leaching of radioisotopes from rocks of the stratum. Hokutolite was previously found crystallizing at an environment of 42–60 °C, and 50 °C appeared to be the favorable temperature [1]. Nevertheless, Table 1 represents that recent temperatures from P7 toward downstream Peito Creek (28.0–31.0 °C) obviously lower (about 3–12 °C) than those recorded in the literature [1]. The aqueous environment was in an oxidative state in light of the redox potentials. Conductivity was related to ionic strength and concentration of electrolytes in geothermal water, which decreased from Geothermal Valley to downstream Peito Creek in this area. Major cations in the water were Fe^{3+}, Pb^{2+}, Sr^{2+}, Ca^{2+} and Ba^{2+} as shown in Table 1. The concentration of Ba^{2+} varied slightly against sampling sites, while that of other major cations declined from the Geothermal Valley toward downstream Peito Creek. Higher ionic concentration in the water led each ion to attract more opposite charge and formed ionic atmosphere surrounding the ions [26], which reduced interionic attraction between cations and anions. Additionally, the temperature at P1–P5 was relatively higher indicating that the ions in water possessed higher kinetic energy than those at other sites and that the dissolution ions was comparatively favorable in this region (P1–P5).

Relative content of Ba and Pb in hokutolite was influenced by their solubility *via* precipitation and complexation [27] with Cl^- and SO_4^{2-} ions. Solution of high acidity supplied concentrated H^+ ions competing the binding of SO_4^{2-} (as the form of HSO_4^-) with Pb^{2+} and Ba^{2+}. This resulted in solubility increase of lead and barium sulfate according to Le Chatelier's principle. Moreover, concentrated

Table 1. Characteristics of the water environment in Peito Hot Spring Area.

Sampling site	Temp. (°C)	pH	E_h (mV)	Conductivity (μS/cm)	TOC (ppm)	Cl^-	SO_4^{2-}	Fe^{3+}	Ca^{2+}	Sr^{2+} (ppm)	Ba^{2+}	Pb^{2+}	[Ba]/[Pb]
P1	68.0	1.38	369	21 030	NA[a]	2400 (75)[b]	2360 (80)	88.8 (3.9)	0.254 (0.008)	0.948 (0.026)	0.075 (0.004)	1.324 (0.050)	0.057 (0.003)
P2	65.8	1.46	367	19 020	NA	2040 (40)	2120 (70)	79.4 (3.5)	0.239 (0.006)	0.896 (0.021)	0.069 (0.003)	1.198 (0.032)	0.060 (0.003)
P3	67.5	1.43	366	18 500	NA	1890 (34)	2030 (43)	67.8 (0.9)	0.218 (0.008)	0.801 (0.022)	0.073 (0.003)	1.028 (0.014)	0.058 (0.003)
P4	68.0	1.47	367	17 370	NA	2283 (47)	2309 (77)	75.4 (1.6)	0.236 (0.007)	0.887 (0.021)	0.070 (0.003)	1.177 (30)	0.071 (0.003)
P5	65.0	1.37	325	21 770	4.71	2480 (75)	2440 (82)	92.2 (3.8)	0.259 (0.007)	0.981 (0.023)	0.085 (0.003)	1.448 (0.028)	0.059 (0.003)
P6	49.0	1.58	353	13 300	4.15	1480 (32)	1500 (42)	54.8 (0.9)	0.180 (0.006)	0.685 (0.019)	0.083 (0.004)	0.890 (0.016)	0.093 (0.004)
P7	31.0	2.29	318	2939	4.75	312 (6)	346 (7)	9.91 (0.15)	0.026 (0.001)	0.121 (0.003)	0.050 (0.003)	0.264 (0.007)	0.190 (0.011)
P8	30.0	2.39	319	2306	4.81	230 (4)	280 (7)	10.4 (0.4)	0.041 (0.001)	0.207 (0.005)	0.065 (0.003)	0.155 (0.003)	0.423 (0.020)
P9	31.0	2.20	320	3425	4.90	346 (6)	394 (10)	11.8 (0.3)	0.054 (0.001)	0.258 (0.006)	0.082 (0.003)	0.265 (0.008)	0.309 (0.014)
P10	31.5	2.20	314	3441	4.80	356 (7)	390 (7)	6.84 (0.06)	0.053 (0.002)	0.259 (0.006)	0.083 (0.003)	0.238 (0.007)	0.349 (0.017)
P11	28.5	2.90	313	872	5.03	85 (2)	126 (3)	2.75 (0.10)	0.027 (0.001)	0.160 (0.004)	0.057 (0.001)	0.060 (0.002)	0.942 (0.041)
P12	28.0	2.61	309	1474	5.21	146 (3)	191 (5)	3.87 (0.04)	0.031 (0.001)	0.174 (0.004)	0.058 (0.001)	0.084 (0.003)	0.689 (0.026)

a: lower than detection limit;
b: two standard deviations.

Cl^- might increase $PbCl_2$ dissolution *via* complexation to produce $PbCl_3^-$ (the logarithm cumulative formation constant, $\log \beta_3 = 18.25$) and $PbCl_4^{2-}$ ($\log \beta_4 = 25.03$) [28]. As the geothermal water flowed into downstream region of the Peito Creek, the temperature lowered and the solubility of $PbSO_4$, $PbCl_2$ and $BaSO_4$ decreased. When water temperature lowered to about 60 °C, the solubility of $BaSO_4$ dropped [29], which enhanced crystal growth of hokutolite by the coprecipitation of Pb^{2+}, Ba^{2+}, Ra^{2+} with SO_4^{2-} [30, 31] as well as the adsorption of plumbian barite on jarosite [$K_2Fe_6(OH)_{12}(SO_4)_4$]. Consequently, hokutolite was discovered at downstream Peito Creek while seldom found in the Geothermal Valley.

On the other hand, the solubility product of $BaSO_4$ (1.1×10^{-10}, at 25 °C) is lower than that of $PbSO_4$ (1.6×10^{-8}, at 25 °C) and $PbCl_2$ (1.7×10^{-5}, at 25 °C), indicating that Ba precipitates prior to Pb when temperature decreases. This should result in a predictable decline for the concentration ratio of Ba to Pb ([Ba]/[Pb]) in water from springhead toward downstream region. In fact, Ba was observed more concentrated than Pb in Hoktolite collected from Peito [7, 32]. According to Table 1, the concentration of Pb in water declined against sampling sites and dropped obviously from P6 toward P12, where the temperature began to decrease. The concentration of Ba, however, varied slightly against the sites. Consequently, the [Ba]/[Pb] ratios increased from springhead toward downstream Peito Creek (Table 1), which was inverse to the theoretically predicted trend. This suggests that human activities had evidently affected water environment of the studied area. The geothermal water had been channeled for several years by neighboring SPA hotels as well as inhabitants from the aquifer and cooled by tap water for hot spring bath. Total organic compounds (TOC) was lower than the detection limit in Geothermal Valley while increased slightly from 4.2 to 5.2 ppm in the creek (P5 toward P12), inferring organic compounds were released along with the discharged waste water. Furthermore, the discharged water also lowered temperature and diluted the concentration of originally existing ions in the water as well. Nevertheless, temperature was found crucial to [Ba]/[Pb] ratios in hokutolite by Sasaki and Minato [33], which was also observed important to those in water according to the increase of [Ba]/[Pb] ratios with decreasing temperature (Table 1).

The estimated ion products (Q) respectively for $PbSO_4$ ($Q(PbSO_4)$), $PbCl_2$ ($Q(PbCl_2)$) and $BaSO_4$ ($Q(BaSO_4)$) all exhibited decline tendency with distance from the springhead (Fig. 2). The tendency of $Q(PbCl_2)$ and $Q(PbSO_4)$ values against sampling sites were both inverse to that of [Ba]/[Pb] ratios (Table 1). In addition, the ion products for $BaSO_4$ were higher than the solubility product constant ($K_{sp}(BaSO_4)$), indicating that Ba was relatively easier precipitated in this region, especially at P6–P10 where hokutolite was discovered. At P1–P5, the values of $Q(PbSO_4)$ were significantly higher than the solubility product constant of $PbSO_4$; however, the chemical parameters (*e.g.*, pH and ionic strength) and complexation reaction occurred in the environment might inhibit the precipitation. The $Q(PbSO_4)$ at P6–P12 and $Q(PbCl_2)$ at all sites were respectively lower than the solubility product constant of $PbSO_4$ and $PbCl_2$, suggesting that $PbSO_4$ and $PbCl_2$ were relatively soluble in this region and accounted for relative content of Ba/Pb in hokutolite from Peito.

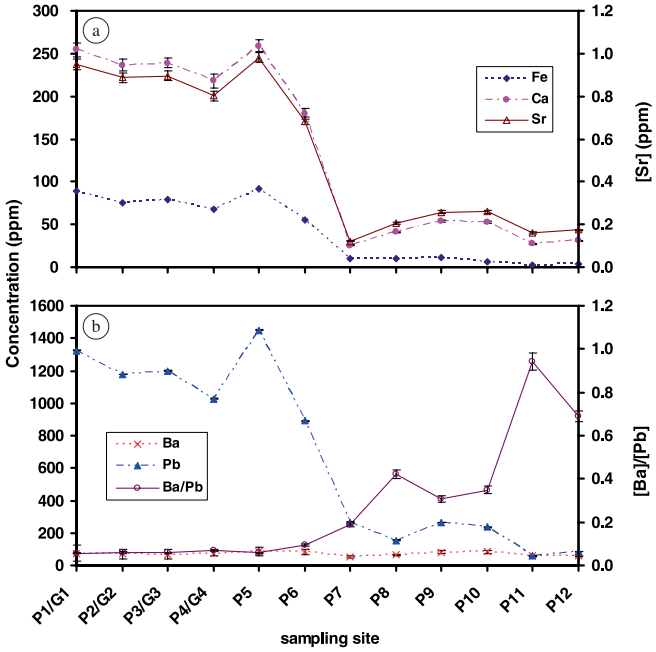

Fig. 2. Variations for (**a**) concentrations (ppm) of Fe, Ca (corresponding to the left ordinate) and Sr (corresponding to the right ordinate) and for (**b**) concentrations (ppm) of Ba and Pb (corresponding to the left ordinate) as well as the [Ba]/[Pb] ratios (corresponding to the right ordinate) against the sampling sites.

3.2 U/Th concentration and its variation with environmental characteristics

The concentration of Th was obviously higher than that of U as illustrated in Fig. 3. Total concentration of U and Th in geothermal water was relatively higher in Geothermal Valley and at upper stream of Peito Creek (P1–P6) than that toward the downstream region (Fig. 3). This phenomenon might be referred to artificial dilution with tap-water. Additionally, U and Th concentrations tended to increase with redox potential (Fig. 3a), indicating that oxidative condition was advantageous for the existence of soluble species of U and Th. The concentration of U was mainly attributed to ^{238}U while that of Th arisen from ^{232}Th according to Eq. (1), in which C_s, W, V, M, t, C_A and N_A denotes concentration (g/L), weight (g), volume (L), molecular weight, half life (a), activity concentration (Bq/L) and Avogadro constant, respectively.

$$C_S = \frac{W}{V} = \frac{C_A M t}{0.693 N_A} \quad (1)$$

Both U and Th concentrations increased linearly with $[Cl^-]$ and $[SO_4^{2-}]$ as demonstrated respectively in Fig. 3b and c, while the influence of major anions was greater on Th than on U in light of the slopes. As plotted in Fig. 3b and c, the concentration ratio of U/Th increased abruptly with either Cl^- or SO_4^{2-} concentrations and reached a maximum about 0.3. The results demonstrated that either U or Th might compound into complexes with Cl^- as well as SO_4^{2-} ions (*e.g.*, UO_2Cl^+, $UO_2(SO_4)_2^{2-}$, $ThCl^{3+}$, $ThCl_3^+$, $ThSO_4^{2+}$, $Th(SO_4)_3^{2-}$ and $Th(SO_4)_4^{4-}$) [34–38], and solubility of Th

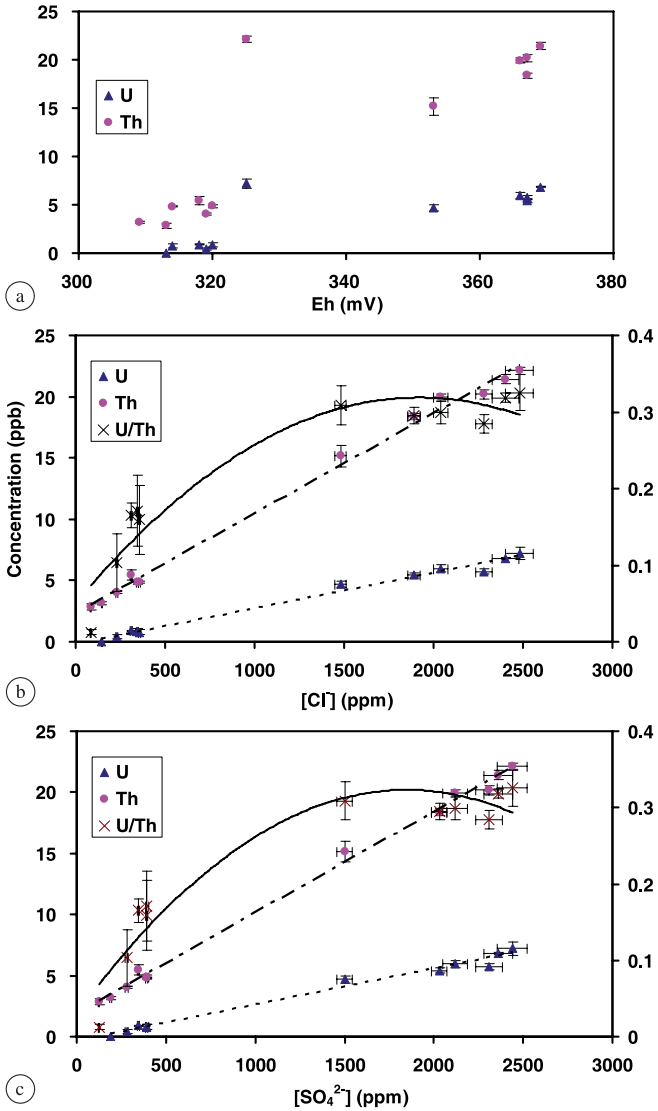

Fig. 3. U/Th concentration *vs.* (**a**) E_h, (**b**) chloride concentration and (**c**) sulfate concentration in water. Both U and Th concentrations increase with chloride (respectively by a relationship of $y = 0.003x - 0.173$ ($R^2 = 0.988$) and $y = 0.0083x + 2.2548$ ($R^2 = 0.9960$); **b**) as well as sulfate concentration (respectively following $y = 0.003x - 0.318$ ($R^2 = 0.986$) and $y = 0.008x + 1.836$ ($R^2 = 0.997$); **c**). The concentration ratio of U/Th relates with chloride concentration in $y = -7 \times 10^{-8}x^2 + 3 \times 10^{-4}x + 0.050$ ($R^2 = 0.918$) and with sulfate concentration in $y = -9 \times 10^{-8}x^2 + 3 \times 10^{-4}x + 0.030$ ($R^2 = 0.9237$).

might be enhanced more obviously than U by complexing with major anions. However, at downstream region from P7 toward P12, the pH increased to > 2.2 and the ionic strength decreased, which enhanced the co-precipitation of U and Th with $Fe(OH)_3$ [34–38].

3.3 Disequilibrium of U-series

The activity concentrations (C_A's) of long-life U-series radionuclides, including ^{238}U, ^{234}U, ^{230}Th and ^{226}Ra, are listed in Table 2. All C_A's of the U-series nuclides in water declined from upstream toward downstream Peito Creek. The C_A's of ^{226}Ra in sediment were apparently higher than those of the long half-life parents (^{238}U, ^{234}U and ^{230}Th), revealing an enrichment of ^{226}Ra in the sediment. Solubility of radium in natural waters is governed by adsorption or precipitation, which is affected by acidity and ionic strength. At conditions with low pH and concentrated ions (*e.g.*, P1–P4), the attraction between radium and other anions as well as the adsorption surface is reduced due to competition of cations (*e.g.*, H^+, Pb^{2+}, Ca^{2+}, Sr^{2+} and Ba^{2+}) with Ra^{2+} [39–41]. Consequently, the C_A's of ^{226}Ra in water reveal decreasing tendency from the springhead toward downstream Peito Creek (P1–P12; Table 2).

3.3.1 Disequilibrium between ^{234}U and ^{238}U

Fig. 4a represents that the radioactivity ratios (ARs) of $^{234}U/^{238}U$ are almost higher than unity (>1), which illustrates slightly disequilibrium in radioactivity. According to the redox potential, the oxidizing condition indicates that soluble uranyl [U(VI)] complexes are stabilized in the sampling area [42]. Because of electron stripping [43] and auto-oxidation effect [44], uranium tends to form UO_2^{2+} or its complexes [45]. Moreover, ascribed to hot atoms produced in the decay process of ^{238}U by Szilárd–Chalmers effect [46–48] as well as the α-recoil energy transfer of a ^{234}U precursor [13, 49, 50], ^{234}U is relatively easier to be leached from damaged site of the lattice. Therefore, most ARs of $^{234}U/^{238}U$ are slightly higher than unity (1.04 ± 0.30–1.38 ± 0.08; except for P1 where AR $= 0.98 \pm 0.07$) as observed.

3.3.2 Disequilibrium between ^{230}Th and ^{234}U

All radioactivity ratios (ARs) of $^{230}Th/^{234}U$ are less than unity (0.23 ± 0.02–0.95 ± 0.11), revealing that ^{234}U is enriched over ^{230}Th. Additionally, the trends of ARs of $^{230}Th/^{234}U$ against major anions are similar. In water, the $^{230}Th/^{234}U$ AR decreases slightly with $[Cl^-]$ and $[SO_4^{2-}]$, while that in sediment shows the inverse trend (Fig. 4a and b). Considering the pH and E_h of the sampling area, U tends to exist in more soluble state (*i.e.*, U(VI), primarily in UO_2^{2+} form) while Th(IV) is the favorable state of thorium [51, 52]. UO_2^{2+} and Th(IV) may further form complexes with Cl^- or SO_4^{2-} [34–38]. The $^{230}Th/^{234}U$ disequilibrium can be ascribed to solubility enhancement of U as the concentration of major anions increases (Fig. 4a and b), which is inverse to the trend of concentration ratio of U/Th in Fig. 3a and b.

3.3.3 Disequilibrium between ^{226}Ra and ^{230}Th

The radioactivity ratios (ARs) of $^{226}Ra/^{230}Th$ against sampling sites are 0.55 ± 0.09–2.27 ± 0.82 in water and 8.21 ± 1.03–18.69 ± 1.78 in sediment (in Fig. 4c and d). Most of the $^{226}Ra/^{230}Th$ ARs are higher than unity, except those in water at P6, P9 and P10, which reveals obvious artificial perturbation by waste water discharge at these sites. No apparent relationship was observed between $^{226}Ra/^{230}Th$ ARs and concentration of major anions.

3.4 Disequilibrium of Th-series

The activity concentrations (C_A's) of Th-series nuclides are higher than that of U-series (Table 2), which is consistent with the observation of background radiation in this area [6]. The trends for C_A's of the long-life Th-series nuclides (including ^{232}Th, ^{228}Ra, and ^{228}Th) in water are similar

Table 2. Activity concentrations of U- and Th-series nuclides in water (P1–P12; unit: pCi/L) and sediment (G1-G4; unit: nCi/kg) of the studied area.

Sampling site	Unit	U-series				Th-series		
		^{238}U	^{234}U	^{230}Th	^{226}Ra	^{232}Th	^{228}Th	^{228}Ra
P 1	pCi/L	2.69	2.64	0.60	1.12	0.74	6.46	10.49
		(0.13)[a]	(0.13)	(0.05)	(0.06)	(0.05)	(0.15)	(0.85)
P 2		2.23	2.37	0.66	1.18	0.72	6.31	8.17
		(0.12)	(0.12)	(0.04)	(0.05)	(0.04)	(0.15)	(0.90)
P 3		2.33	2.59	0.66	1.24	0.71	5.99	8.33
		(0.12)	(0.13)	(0.08)	(0.04)	(0.08)	(0.23)	(1.05)
P 4		2.08	2.24	0.70	1.19	0.69	6.63	7.90
		(0.12)	(0.13)	(0.04)	(0.06)	(0.04)	(0.12)	(0.61)
P 5		1.73	2.38	0.86	1.49	0.90	9.26	8.87
		(0.07)	(0.07)	(0.06)	(0.06)	(0.06)	(0.18)	(0.71)
P 6		1.01	1.12	0.53	0.44	0.57	4.99	7.74
		(0.07)	(0.07)	(0.08)	(0.04)	(0.08)	(0.23)	(0.77)
P 7		0.32	0.35	0.30	0.37	0.31	2.74	7.62
		(0.04)	(0.04)	(0.07)	(0.02)	(0.07)	(0.21)	(0.77)
P 8		0.31	0.41	0.16	0.30	0.17	1.78	6.76
		(0.05)	(0.05)	(0.03)	(0.02)	(0.03)	(0.09)	(0.39)
P 9		0.37	0.45	0.27	0.17	0.29	3.11	6.61
		(0.04)	(0.05)	(0.03)	(0.02)	(0.03)	(0.11)	(0.72)
P 10		0.34	0.43	0.31	0.17	0.31	3.46	6.27
		(0.05)	(0.06)	(0.05)	(0.01)	(0.05)	(0.15)	(0.42)
P 11		0.09	0.10	0.07	0.17	0.06	0.43	6.01
		(0.02)	(0.02)	(0.03)	(0.01)	(0.02)	(0.06)	(0.41)
P 12		0.16	0.20	0.16	0.20	0.12	0.95	6.11
		(0.03)	(0.03)	(0.03)	(0.01)	(0.03)	(0.07)	(0.42)
G1	nCi/kg	1.22	1.26	1.19	10.33	1.88	27.62	74.59
		(0.07)	(0.05)	(0.13)	(0.51)	(0.06)	(0.49)	(0.16)
G2		1.45	1.52	0.74	6.11	1.12	27.86	35.68
		(0.07)	(0.05)	(0.08)	(0.39)	(0.10)	(0.49)	(0.11)
G3		1.08	1.13	0.56	10.52	0.68	74.59	117.03
		(0.08)	(0.08)	(0.05)	(0.49)	(0.05)	(0.54)	(0.24)
G4		1.14	1.20	0.76	8.47	0.92	21.66	89.76
		(0.06)	(0.06)	(0.08)	(0.44)	(0.06)	(0.40)	(0.22)

a: Two standard deviations.

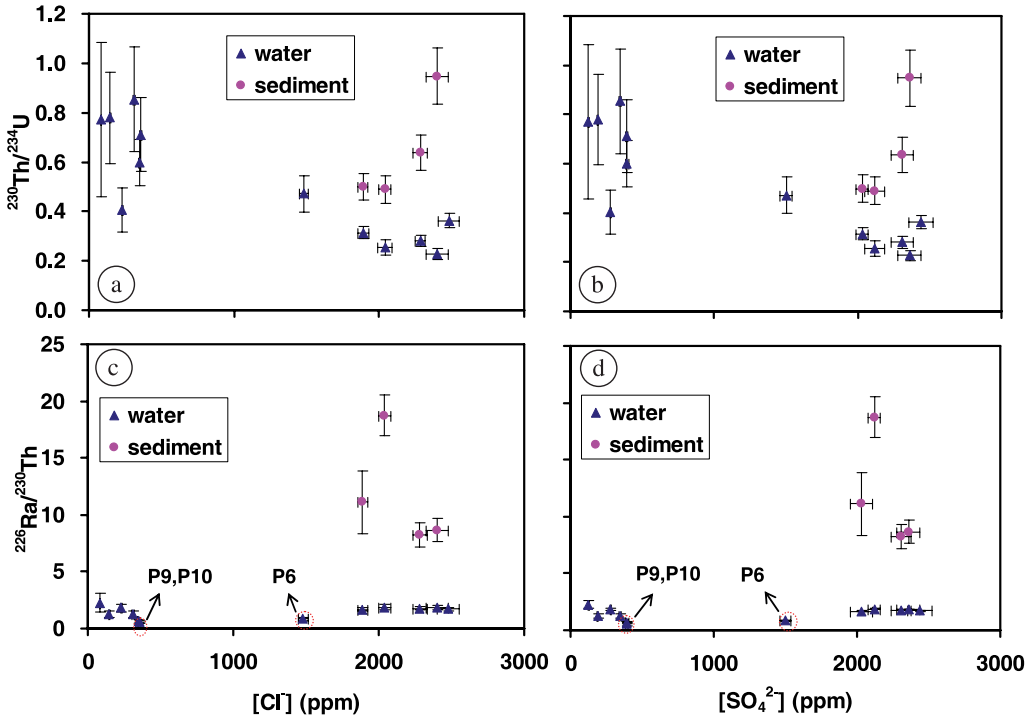

Fig. 4. Variations for disequilibria between long-life U-series radionuclides and characteristics of the water environment in Peito Hot Spring Area. The ratios of ^{226}Ra/^{230}Th are higher than unity except those at P6 (0.83 ± 0.14), P9 (0.64 ± 0.11) and P10 (0.55 ± 0.09) as indicated in (**c**) and (**d**).

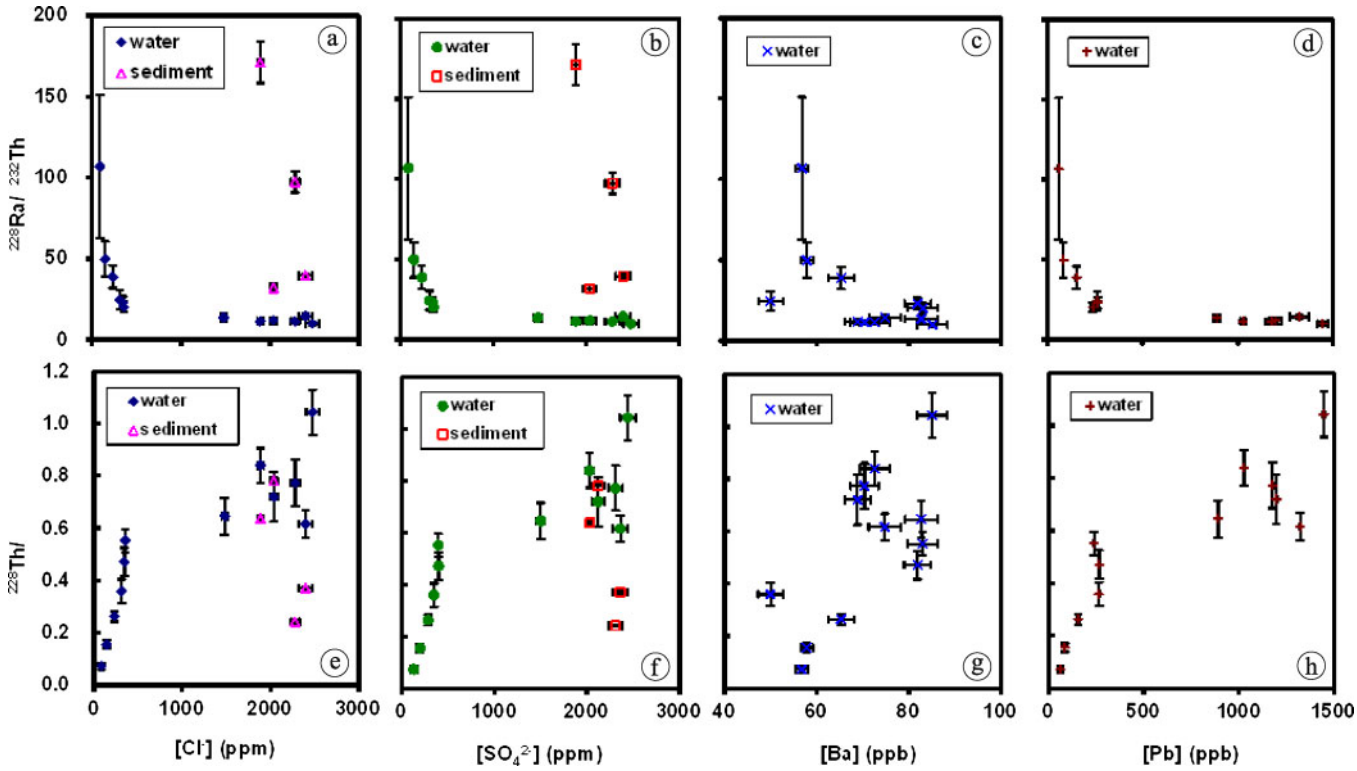

Fig. 5. Variation for ARs of ^{228}Ra/^{232}Th and ^{228}Th/^{228}Ra with concentration of Cl^-, SO_4^{2-}, Ba^{2+} and Pb^{2+} ions.

to those of U-series, which decline from upstream toward downstream Peito Creek attributed to the decrease of acidity and ionic strength.

3.4.1 Disequilibrium between ^{228}Ra and ^{232}Th

^{228}Ra is much more enriched over ^{232}Th either in water or sediment, resulting in manifest disequilibrium between ^{228}Ra and ^{232}Th. The ARs of ^{228}Ra/^{232}Th are 9.86 ± 1.04–106.8 ± 44.3 in water and 31.73 ± 2.82–171.2 ± 12.9 in sediment. With increasing Cl^- concentration, the ^{228}Ra/^{232}Th ARs in water decrease obviously due to complexation of Th with Cl^- ions, which increases the solubility of thorium [Figs. 3b and 5a]. On the other hand, the ^{228}Ra/^{232}Th ARs in water decrease abruptly with SO_4^{2-} concentrations (Fig. 5b), which is consistent with the trend of ^{228}Ra/^{232}Th ARs *vs.* the concentration of Ba (Fig. 5c) and Pb (Fig. 5d), respectively. This results can be accordingly ascribed to the co-precipitation of radium with $(Ba,Pb)SO_4$ ($K_{sp} = 1.1 \times 10^{-10}$ for $BaSO_4$ and 1.8×10^{-8} for $PbSO_4$ at 25 °C [53]) and complexation of Th with SO_4^{2-} ions; however, effect of the former is greater than that of the later (Fig. 5b) since Th forms soluble complex ions (logarithm formation constant is 12.4 for $Th(SO_4)_3^{2-}$ [54]) when the concentration of SO_4^{2-} ions increases. No apparent tendency was observed between ^{228}Ra/^{232}Th AR in sediment and the concentration of major anions in water of the Geothermal Valley.

3.4.2 Disequilibrium between ^{228}Th and ^{228}Ra

Variations of ^{228}Th/^{228}Ra ARs in water and in sediment with Cl^- and SO_4^{2-} ions were illustrated in Fig. 5e and f, respectively. Nearly all ^{228}Th/^{228}Ra ARs are less than unity. At lower Cl^- and SO_4^{2-} concentrations, the disequilibrium between ^{228}Th and ^{228}Ra in water is more obvious. When concentrations of Cl^- and SO_4^{2-} increase, the AR of ^{228}Th/^{228}Ra in water (0.07 ± 0.01–1.04 ± 0.09) raises and approaches unity. No apparent relationship between ^{228}Th/^{228}Ra ARs (0.24 ± 0.00–0.78 ± 0.01) in sediment and concentration of major anions was discovered. Furthermore, the ^{228}Th/^{228}Ra ARs in water also rise with Ba and Pb concentrations as illustrated respectively in Fig. 5g and h. This phenomenon is due to chemical selection *via* co-precipitation of Ra with $(Ba,Pb)SO_4$ [30] and Th complexation with major anions, as discussed in the disequilibrium between ^{228}Ra and ^{232}Th.

3.4.3 Disequilibrium between ^{228}Th and ^{232}Th

In water, the activity concentrations (C_A's; pCi/L) of ^{228}Th are similar to that of ^{232}Th, which exhibit a trend declining against sampling sites (Table 2). However, the C_A's of ^{228}Th are much higher than those of ^{232}Th, which leads to evident disequilibrium between ^{232}Th and ^{228}Th with ARs of 7.69 ± 1.70–11.14 ± 1.72 in water and 14.66 ± 0.51–109.09 ± 8.23 in sediment. Since ^{228}Th and ^{232}Th have the same chemical speciation, the disequilibrium should not be ascribed to chemical reactions they involved. During the decay of ^{232}Th in the rock or sediment, ^{228}Ra may obtain α-recoil energy and thus easier to be leached than its parent. As a progeny of ^{228}Ra, ^{228}Th may immigrate into geofluid by decay from dissolved ^{228}Ra in water. Accordingly, ^{228}Th can be more soluble than ^{232}Th in the water environment resulting in ^{228}Th/^{232}Th ARs apparently > 1. Moreover, the ^{228}Th/^{232}Th ARs in sediment (at G1–G4) of Geothermal Valley seem to elevates with the C_A's of ^{228}Ra decayed from ^{232}Th in sediment in a relationship of a third degree polynomial (Fig. 6).

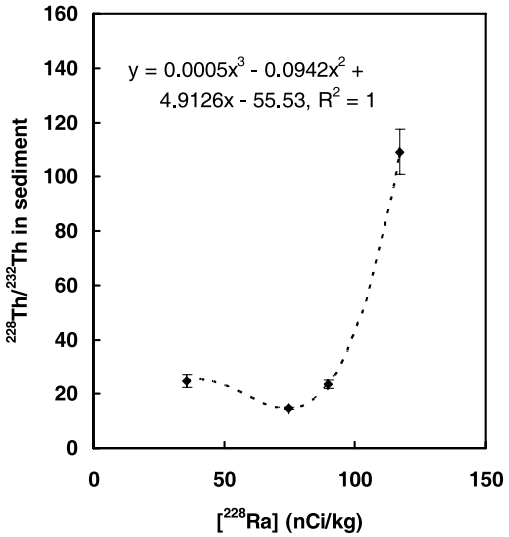

Fig. 6. Variation for ARs of $^{228}Th/^{232}Th$ with activity concentrations of ^{228}Ra in sediment.

This result indicates that the $^{228}Th/^{232}Th$ AR in sediment increases drastically with the C_A's of ^{228}Ra in sediment, which reveals an effect of α-recoil on the disequilibrium between ^{228}Th and ^{232}Th in sediment.

3.5 Derivation for the formation of hokutolite *via* migration and radiochemistry of the radionuclides

According to the effect of characteristics of water environment on the C_A's and disequilibria between radionuclides of U- and Th-series, the processes and radiochemistry with respect to the formation of hokutolite in Peito can be proposed as demonstrated in Fig. 7. The primordial nuclides, ^{238}U and ^{232}Th, of U- and Th-series respectively can be leached from the rock by acid and immigrate into the geothermal water (path A and a) or alternatively decay in the rock into the next long-life progeny (*i.e.*, ^{234}U and ^{228}Ra, respectively) (path B and b). In the acidic and oxidizing environment of the studied area, ^{238}U is likely to appear in a hexavalent state resulting from auto-oxidation and electron stripping (path C), which then decay consecutively into ^{234}U as a uranyl form ($^{234}UO_2^{2+}$; path D). The ^{234}U in rock of the stratum may also be dissolved in water in $^{234}UO_2^{2+}$ form (path E). Once the acidity of the water environment increases or the E_h decreases, the valence state of uranium may change and the migration of uranium *via* path C, D and E can be altered. In further decay, the ^{234}U transforms successively into ^{230}Th and ^{226}Ra either in water (path F and I) or rock (path G and J). The migration of ^{230}Th among water, rock and sediment is affected by acidity, redox potential or concentrations of Cl^- and SO_4^{2-} ions of the aqueous environment (path H). The change of water chemistry can thus influence path H. ^{226}Ra and ^{228}Ra in the rock can immigrate into the water (path K and d), and some of which subsides into the sediment. The soluble radium can be coprecipitated with plumbian barite (path L and g) and adsorbed on jarosite as hokutolite (path M). Precipitation/dissolution of ^{226}Ra and ^{228}Ra is governed by acidity and ionic strength. Therefore, the change in pH and ionic strength of the water environment can interfere path L, M and g. ^{228}Ra, either in water or rock, may further decay into ^{228}Th (path c and e). Migration of the daughter, ^{228}Th, among water, rock and sediment is identical to that of ^{230}Th (path f). Co-precipitation of U and Th with $Fe(OH)_3$ occurs after the precipitation of plumbian barite (path N) [34]. Accordingly, based on the paths for the formation of hokutolite derived in this study, the quality of the water environment is critical for the migration of radionuclides, which can further determine the formation and conservation of hokutolite.

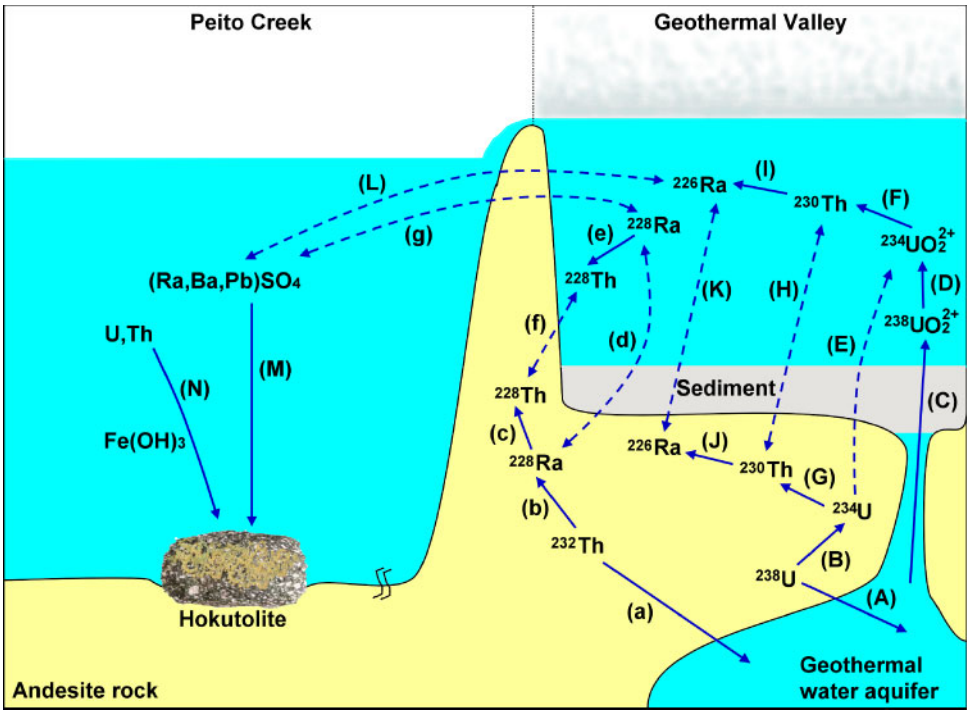

Fig. 7. The formation of hokutolite derived from migrations of U- and Th-series nuclides among rock of the stratum, geothermal water and sediment as a result of chemical reactions and radiochemical processes occurring in the studied area.

3.6 Suggestion for hokutolite conservation

The environment of Peito Hot Spring Area where hokutolite was discovered has been devastated since 1960s. In these two decades, the environmental condition is worse. To effectively achieve the goal of hokutolite recovery, legislation is imperative for protecting this precious mineral as well as its environment. Well drilling and pipeline constructing in this area are suggested to be restrained.

4. Conclusion

The water environment was characterized as acidic, oxidative, highly electrolytic and high in concentrations of with Cl^- and SO_4^{2-} ions. The acidity, E_h, temperature and Cl^-/SO_4^{2-} concentration were decreasing from Geothermal Valley toward downstream Peito Creek, indicating that Geothermal Valley was relatively favorable to form hokutolite. Both the temperature decrease compared with historical records at downstream Peito Creek and the [Ba]/[Pb] ratios against sampling sites illustrated obvious effect of human activities on aqueous environment of the studied area. The comparison between ion products and solubility products revealed that $PbSO_4$ and $PbCl_2$ were relatively soluble, which were responsible for Ba/Pb ratio in hokutolite from Peito.

Both U and Th concentrations in geothermal water increased with E_h. The solubility of U and Th was increased by forming complex with Cl^- as well as SO_4^{2-} ions, while the effect was greater on Th. At downstream region where pH increased to > 2.2 and the ionic strength decreased, the co-precipitation of U and Th with $Fe(OH)_3$ was enhanced. All C_A's of nuclides of the U- and Th-series in water declined from springhead toward downstream area. Obvious enrichment of ^{226}Ra in sediment as well as ^{228}Ra both in water and sediment were revealed. ARs of $^{234}U/^{238}U$ were almost higher than unity ascribed to Szilárd–Chalmers effect and α-recoil energy transferred to ^{234}U. All ARs of $^{230}Th/^{234}U$ were less than unity attributed to that ^{234}U forms more soluble species than ^{230}Th does. No apparent relationship existed between $^{226}Ra/^{230}Th$ ARs in water and concentration of major anions. The C_A of ^{228}Ra as well as ^{226}Ra was affected by pH, E_h and SO_4^{2-} concentration. Obvious disequilibria between ^{228}Th and ^{232}Th as well as evident enrichment of ^{228}Th were observed both in water and in sediment attributed to α-recoil energy obtained by ^{228}Ra. Nearly all $^{228}Th/^{228}Ra$ ARs were less than unity. Disequilibria of $^{228}Ra/^{232}Th$ was apparent, and the $^{228}Ra/^{232}Th$ AR in water related to complexation of Th with major anions as well as co-precipitation of radium with $(Ba,Pb)SO_4$. ^{228}Ra enrichment attributed to α-recoil resulted in evident disequilibria between ^{232}Th and ^{228}Th.

The processes and radiochemical reactions were derived and illustrated from this study to expound the migration and disequilibria of long-life radionuclides. Furthermore, the pathways in the formation of hokutolite deduced from this work can be applied to the conservation of hokutolite in Peito.

Acknowledgment. The authors would like to show their appreciation for the help in chemical analysis from Institute of Nuclear Energy Research (INER, R.O.C) by Gia-Luen Guo and Yi-Feng Jiang of the Cellulose Bioethanol Project research group as well as Haw-Jen Wu, Ho-Chuan Huang, Tsan-Yuh Yang, Tzung-Yi Lin and Tsung-Yuan Wang of the Chemical Analysis Division. Assistances of sampling from Tin-Yi Lu is deeply acknowledged. This paper is also written to commemorate Jun-Nan. Tsai, who assisted the collection of the samples.

References

1. Chang, F. H.: Genetic study of anglesobarite from Peitou, Taiwan. Acta Geol. Taiwan. **9**, 7 (1961).
2. Huang, C. W.: Measurement of radioactivity at Peito Hot Spring and analysis of Rn-222 in hot springs in Taiwan. In: *International Conference on Centennial of Discovering Hokutolite and Hot Springs*. Taipei, Taiwan, 7–8 October (2005), p. 147.
3. Hayakawa, M., Nakano, T.: The radioactive constituents of the sediments from the springs of Hokuto, Taiwan. Z. Anorg. Chem. **78**, 183 (1912).
4. Spencer, L. T.: A list of new mineral names. Mineral Mag. **17**, 334 (1916).
5. Weng, P. S., Chu, T. C.: Natural radiation background in Metropolitan Taipei. J. Radiat. Res. **32**, 165 (1991).
6. Chen, C. J., Lin, P. H., Huang, C. C.: High background radiation valley formed by Peitou Hot Spring. Int. Congress Ser. **1276**, 315 (2005).
7. Momoshima, N., Nita, J., Maeda, Y., Sugihara, S., Shinno, I., Matsuoka, N., Huang, C. W.: Chemical composition and radioactivity in hokutolite (plumbian barite) collected at Peito Hot Spring, Taiwan. J. Environ. Radioact. **37**(1), 85 (1997).
8. Weng, P. S.: Natural radionuclides and radiation doses in Taiwan. Nucl. Sci. J. **25**(3), 189 (1988).
9. Bourdon, B., Bureau, S., Andersen, M. B., Pili, E., Hubert, A.: Weathering rates from top to bottom in a carbonate environment. Chem. Geol. **258**(3–4), 275 (2009).
10. Guibert, P., Lahaye, C., Bechtel, F.: The importance of U-series disequilibrium of sediments in luminescence dating: a case study at the Roc De Marsal Cave (Dordogne, France). Radiat. Meas. **44**, 223 (2009).
11. Ivanovich, M.: Aspects of uranium/thorium series disequilibrium applications to radionuclide migration studies. Radiochim. Acta **52/53**:257 (1991).
12. Ivanovich, M.: Uranium series disequilibrium: concepts and applications. Radiochim. Acta **64**, 81 (1994).
13. Kigoshi, K.: Alpha-recoil thorium-234: dissolution into water and the uranium-234/uranium-238 disequilibrium in nature. Science **173**, 47 (1971).
14. Kozłowska, B., Morelli, D., Walencik, A., Dorda, J., Altamore, I., Chieffalo, V., Giammanco, S., Immè, G., Zipper, W.: Radioactivity in waters of Mt. Etna (Italy). Radiat. Meas. **44**, 384 (2009).
15. Maiti, K., Benitez-Nelson, C. R., Lomas, M. W., Krause, J. W.: Biogeochemical responses to late-winter storms in the Sargasso Sea, III – estimates of export production using ^{234}Th:^{238}U disequilibria and sediment traps. Deep-Sea Res. Pt. I **56**, 875 (2009).
16. Michael, C. T., Hein, A., Zacharias, N., Kritidis, P.: Disequilibrium estimations in the U and Th series by using thick source alpha-particle spectroscopy. Radiat. Meas. **43**, 1149 (2008).
17. Pérez-Peña, J. V., Azañón, J. M., Azor, A., Tuccimei, P., Seta, M. D., Soligo, M.: Quaternary landscape evolution and erosion rates for an intramontane Neogene basin (Guadix–Baza basin, SE Spain). Geomorphology **106**, 206 (2009).
18. Roberts, H. M., Plater, A. J.: U- and Th-series disequilibria in coastal infill sediments from Praia da Rocha (Algarve Region, Portugal): a contribution to the study of late Quaternary weathering and erosion. Geomorphology **26**, 223 (1999).
19. Sun, H., Semkow, T. M.: Mobilization of thorium, radium and radon radionuc1ides in ground water by successive alpha-recoils. J. Hydrol. **205**, 126 (1998).
20. Lin, C. C., Chu, T. C., Huang, Y. F.: Disequilibria in the disintegration series of U and Th and chemical parameters in thermal spring waters from the Tatun volcanic area (Taiwan). Radiochim. Acta **91**, 403 (2003).
21. Wang, J. J.: *Studies of the migration and distribution of naturally occurring radionuc1ides in hot spring and river waters within the Tatun Volcano Group Area*. Ph.D. Dissertation, National Tsing Hua University, Hsinchu, Taiwan (1994), pp. 146–182.

22. Weng, P. S., Tsai, C. M.: Radium-226 concentrations in Taiwan hot spring and river waters. Health Phys. **24**, 429 (1973).
23. Kim, Y. J., Kim, C. K., Kim, C. S., Yun, J. Y., Rho, B. H.: Determination of ^{226}Ra in environmental samples using high-resolution inductively coupled plasma mass spectrometry. J. Radioanal. Nucl. Chem. **240**(2), 613 (1999).
24. Parsa, B., Obed, R. N., Nemeth, W. K., Suozzo, G. P.: U determination of gross alpha, ^{224}Ra, ^{226}Ra, and ^{228}Ra activities in drinking water using a single sample preparation procedure. Health Phys. **89**(6), 660 (2005).
25. Tsai, T. L., Lin, C. C., Chu, T. C.: Micro-column solid phase extraction to determine uranium and thorium in environmental samples. Appl. Radiat. Isot. **66**, 1097 (2008).
26. Harris, D. C.: *Exploring Chemical Analysis*. 3rd Edn., W.H. Freeman and Company, New York (2004), p. 136.
27. Watanuki, K.: Geochemistry of hokutolite in Peitou, Tamagawa and thermal water producing the mineral. In: International Conference on Centennial of Discovering Hokutolite and Hot Springs. Taipei, Taiwan, 7–8 October (2005), p. 8.
28. Ngila, J. C., Silavwe, N., Kiptoo, J. K., Thabano, J. E. R.: Voltammetric investigation of the distribution of hydroxo-, chloro-, EDTA and carbohydrate complexes of lead, chromium, zinc, cadmium and copper: potential application to metal speciation studies in brewery wastewater. Bull. Chem. Soc. Ethiop. **19**(1), 125 (2005).
29. Langmuir, D., Riese, A. C.: The thermodynamic properties of radium. Geochim. Cosmochim. Acta. **49**, 1593 (1985).
30. Tim, G., Mike, C.: Geochemical factors controlling radium activity in a sandstone aquifer. Ground Water **44** (4), 518 (2006).
31. Chao, J. H., Chuang, C. Y., Yeh, S. A., Wu, J. M.: Relationship between radioactivity of radium and concentrations of barium and lead in hokutolite. Appl. Radiat. Isot. **67**, 650 (2009).
32. Yamamoto, M., Tomita, J., Sakaguchi, A., Shirotori, T., Shiraki, K., Tazaki, K.: Radiochemical aspect of hokultolite collected recently at Peito Hot Spring, Taiwan. In: International Conference on Centennial of Discovering Hokutolite and Hot Springs. Taipei, Taiwan, 7–8 October (2005), p. 64.
33. Sasaki, N., Minato, H.: Relationship between lattice constants and strontium and calcium contents of hokutolite. Mineral. J. **11**, 62 (1982).
34. Langmuir, D.: Uranium solution-mineral equilibria at low temperatures with applications to sedimentary ore deposits. Geochim. Cosmochim. Acta **42**, 547–569 (1978).
35. Langmuir, D., Herman, J. S.: The mobility of thorium in natural waters at low temperatures. Geochim. Cosmochim. Acta **44**, 1753 (1980).
36. Hennig, C., Ikeda, A., Schmeide, K., Brendler, V., Moll, H., Tsushima, S., Scheinost, A. C., Skanthakumar, S., Wilson, R., Soderholm, L., Servaes, K., Gorrler-Walrand, C., Van Deun, R.: The relationship of monodentate and bidentate coordinated uranium(VI) sulfate in aqueous solution. Radiochim. Acta **96**, 607 (2008).
37. Hennig, C., Kraus, W., Emmerling, F., Ikeda, A., Scheinost, A. C.: Coordination of a uranium(IV) sulfate monomer in an aqueous solution and in the solid state. Inorg. Chem. **47**, 1634 (2008).
38. Altmaier, M., Neck, V., Fanghänel, T.: Solubility and colloid formation of Th(IV) in concentrated NaCl and $MgCl_2$ solution. Radiochim. Acta **92**, 537 (2004).
39. Tomita, J., Sakaguchi, A., Yamamoto, M.: Hokutolite collected from riverbed at Peitou Hot Spring in Taiwan: with emphasis on radiochemical studies. J. Radioanal. Nucl. Chem. **270**, 567 (2006).
40. Grund, T., Cape, M.: Geochemical factors controlling radium activity in sandstone aquifer. Ground Water **44**(4), 518 (2006).
41. Riese, A. C.: Adsorption of radium and thorium onto quartz and kaolinite: A comparison of solution/surface equilibria model. Ph.D. dissertation, Colorado School of Mines, Golden (1982).
42. Battye, D. L., Ashman, P. J.: An Assessment of Radiological Hazards in Hot Rock Geothermal Systems. CHEMENGTEST Consulting Report 2008/2314-1, Adelaide University, Australia (2008), p. 5.
43. Rosholt, J. N., Shields, W. R., Garner, E. L.: Isotope fraction of uranium in sandstone. Science **139**, 224 (1963).
44. Ellsworth, H. V.: Rare-Earth Minerals of Canada, Geological Survey of Canada. Econ. Geol. Ser. **11**, 272 (1932).
45. Choppin, G R. Liljezin, J. O., Rydberg, J.: *Radiochemistry and Nuclear Chemistry*. 2nd Edn., Butterworth-Heinemann Ltd., Oxford (1995), p. 655.
46. Cherdyntsev, V. V., Chalov, P. I., Khaidarov, G. Z.: Transactions of the Third Session of the Committee for Determination of Absolute Ages of Geologic Formations. Izv. Akad. Nauk. SSSR (1955), p. 175.
47. Baranov, V. I., Surkov, Y. A., Vilinskii, V. D.: Isotopic shift in natural uranium compounds. Geochem. (USSR) **5**, 591 (1958).
48. Thurber, D. L.: Anomalous $^{234}U/^{238}U$ in nature. J. Geophys. Res. **67**, 4518–4520 (1962).
49. Adloff, J. P., Roessler, K.: Recoil and transmutation effects in the migration behavior of actinides. Radiochim. Acta **52**/**53**, 269 (1991).
50. Fleischer, R. L., Raabe, O. G.: Recoiling alpha-emitting nuclei: mechanisms for uranium series disequilibrium. Geochim. Acta **42**, 973 (1978).
51. Focazio, M. J., Szabo, Z., Kraemer, T. F., Mullin, A. H., Barringer, T. H., de Paul, V. T.: Occurrence of selected radionuclides in ground water used for drinking water in the United States, a reconnaissance survey, 1998: U.S. In: Geological Survey Water-Resources Investigations Report WRI 00-4273 (2001), p. 39.
52. Zapecza, O. S., Szabo, Z.: Natural radioactivity in ground water – a review. In: *National Water Summary 1986 – Hydrologic Events and Ground-Water Quality*. (Moody, D. W., Carr, J., Chase, E. B., and Paulson, R. W., eds.) US Geological Survey, Water-Supply Paper 2325 (1987), p. 50.
53. Moore, J. W., Stanitski, C. L., Jurs, P. C.: *Principles of Chemistry: The Molecular Science*. 1st Edn., Thomson Brooks/Cole Publication Co. (2010), p. 595.
54. Borkowski, M., Richmann, M.: *Comparison of Recent Thorium Thermodynamic Data with Those Used in the WIPP FMT_050405.chemdat Database*, LANL-CO ACRSP ACP-0911-01-03-01, Los Alamos National Laboratory (2009).